RAL-5129
RREZ-015G

The Precise Measurement of Internal Stresses Within Materials using Pulsed Neutrons,

by

M W Johnson[a], L Edwards[b], H G Priesmeyer[c],

F Rustichelli[d] & P J Withers[e]

a) ISIS Facility, Rutherford Appleton Laboratory, Chilton, Didcot, Oxon OX11 0QX, UK
b) Fracture Research Group, Materials Discipline, The Open University MILTON KEYNES, MK7 6AA, UK
c) c/o GKSS Research Centre, Max-Planck-Str. 1, D-21502 Geesthacht, GERMANY
d) Istituto di Scienze Fisiche, Facoltà di Medicina e Chirurgia, Universi tà degli Studi di Ancona, Via Ranieri Monte d'Ago, 60131 Ancona, ITALY
e) Department of Materials Science & Metallurgy, University of Cambridge, Pembroke Street, CAMBRIDGE CB23QZ, UK

1 Abstract

Residual stresses in engineering components are often major factors in determining the life of the component. Traditional methods of determining residual stresses are either limited to surface measurements, or are destructive in nature. The objective of The *PREMIS* project has been to develop a routine, non destructive method of measuring internal stresses deep within engineering materials and components. This has been achieved through the construction of a new instrument, ENGIN, on the pulsed neutron facility ISIS, at the Rutherford Appleton Laboratory, and the development of the neutron strain scanning technique using this instrument.

ENGIN is a custom designed neutron diffractometer which is able to measure the internal strain (and hence stress) by determining the change in the lattice spacings between the atoms within the material under study. The significant advantage of the neutron measurement is the ability of the neutron to penetrate many centimetres into most common engineering materials (steels, aluminium, MMCs, etc...) thus making measurements deep within the material possible. A further advantage of the *pulsed* neutron technique used on ENGIN is its ability to record the lattice spacings of each phase of a composite material simultaneously - thus providing a unique insigh: into the stresses present in a composite component.

The PREMIS programme has developed the technique of neutron strain scanning by studying the following areas:

- thermal cycling of composites
- stress gradients in reactor walls
- fatigue cracks in MMCS
- adhesive joints
- test of residual stress relief procedures
- coId expanded fast ener holes
- development of strain standards

The PREMIS consortium has drawn upon expertise in Germany, Italy and the UK to construct the instrument, write new software and demonstrate the technique's full (capabilities.

2 Introduction

A new instrument for neutron strain scanning, ENGIN, has been built at the pulsed neutron source ISIS Rutherford Appleton Laboratory, UK. This technique is now being explored through a series of measurements devised to establish its capabilities. The project is being jointly undertaken by researchers from Germany (Kiel), Italy (Ancona) and the UK (Cambridge, Open University and RAL).

All engineering components are stressed to some extent, either in-service or as a result of their manufacture. Such stresses can result in mechanical failure, which may be costly to industry and have significant safety implications. In these cases, often found in the aerospace, automobile or nuclear industries, a deeper understanding of the stresses within a component is required.

It is to solve this problem that a new instrument (ENGIN) capable of measuring elastic strain variations under these conditions, up to 50 mm beneath the surface of engineering metals and ceramics has been built at the Rutherford Appleton Laboratory (UK) [1]. The technique, called *neutron strain scanning* (NSS), uses the crystal lattice within most engineering materials as an atomic strain gauge to measure strain distributions with a sub-millimetre spatial resolution to an accuracy of better than 50 microstrain. The success of the method lies in the fact that it uses a neutron beam that is many more times penetrating than conventional X-rays. While the technique of neutron strain measurement has been developed considerably since its inception in 1980 [2], this has largely been on continuous, reactor neutron sources [3]. However, pulsed neutron sources using the time-of-flight method, offer potential advantages in measuring internal strains, especially in composite materials.

The ENGIN instrument is the first instrument using the *pulsed-neutron* technique in the world designed and optimised exclusively for making measurements on engineering components. These can be up to about a metre in size, and weigh as much as 250 kg.

There are thus many advantages of NSS over conventional stress measurement techniques:

- it can provide sub-surface information not obtainable by any other non-destructive non-contacting technique,
- it is applicable to most crystalline materials,
- *the pulsed* neutron strain scanning can measure the strain in *each component* of a composite material simultaneously within the same gauge volume,
- complicated data corrections are not required, since the stress state is not disturbed by the 'measurement,
- it can be used to measure stresses within components in environments typical of those experienced in-service,
- it can be used to validate finite element simulations and thus improve performance or lifetime predictions,
- it is much faster and less labour intensive than conventional destructive methods, such a hole drilling or X-ray diffraction followed by surface removal.

The main disadvantage of the technique lies in the scarcity of strain scanning facilities. However, the instrument and expertise at the Rutherford Appleton Laboratory now provide new access within Europe to industry.

The construction of the ENGIN pulsed neutron strain scanner was only the first part of the PREMIS 'project. Most importantly the instrument was then used to develop the technique through studying a range of engineering problems. In doing so, the technique has been refined, the correct software has been developed, and new results in engineering science obtained. Below, in section 3, we describe the method and the instrument in more detail, and in section 4 the new results obtained.

3 Technical Description

3.1 Design *Objectives of the ENGIN instrument*

The neutron strain scanning (NSS) technique, like its X-ray counterpart, determines the strain in a material by measuring the distance d_{hkl} between the {hkl} lattice planes within a small volume of the sample - the gauge volume. The strain is then Calculated by comparing this measurement with that of the un-strained material (d_0).

ENGIN, a pulsed neutron strain scanning instrument, is therefore a specialised neutron diffractometer with three important attributes:

- an ability to measure the atomic lattice spacings to a high precision
- an ability to make such measurements on a small 'gauge volume' within the sample under study, and
- an ability to position the gauge volume accurately with the sample.

Moreover, by rotating the sample the strain may be measured along any particular direction, thus enabling the *vector* strain field to be mapped out in 3-dimensions.

In designing an instrument to meet the three objectives listed above a number of principal design parameters were decided upon:

- strain withii samples could be measured to +50 .10-6 (+50 με)
- . gauge volumes within samples could be resolved down to <2mm cube
- samples could be scanned ± 13cm (x,y,z)
- . samples could be positioned to ± 0.1 mm
- samples could weigh up to 250 kg
- samples temperatures could be controlled up to 1000K

3.2 *Neutron Diffraction*

The ENGIN instrument is situated on the S9 beamline at the. ISIS pulsed neutron source, situated at the Rutherford Appleton Laboratory, UK. To understand its operation it is necessary to describe briefly the technique of pulsed neutron diffraction.

A diffractometer on a "pulsed neutron source, is shown diagramatically in Fig.1. Neutrons originate from the moderator (M) in short pulses and travel to the sample (S) where they may scatter into a detector (D) situated at an angle of 2θ to the incident beam. The neutrons have a wide energy range from a few meV up to many eV. Such energies correspond to neutrons with velocities comparable to the speed of sound, and hence the neutrons take a few milliseconds to travel from the moderator to the detector, a distance of approximately 15m.

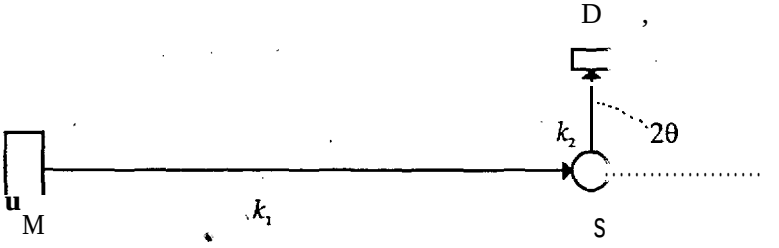

Fig. 1 ***A*** *schematic layout of a pulsed neutron diffractometer.*

A polycrystalline sample, such as most metal engineering components, will diffract only those neutrons that satisfy Bragg's law;

$$\lambda = 2|d|\sin\theta \qquad 3.1$$

and if the detected neutron count is plotted as a function of time (Fig. 2) it will exhibit a series of peaks corresponding to the different d_{hkl} lattice planes in the material. By measuring the time-of-flight (t) from the moderator to the detector, the velocity (v) of the neutrons contributing to a particular Bragg peak may be calculated.

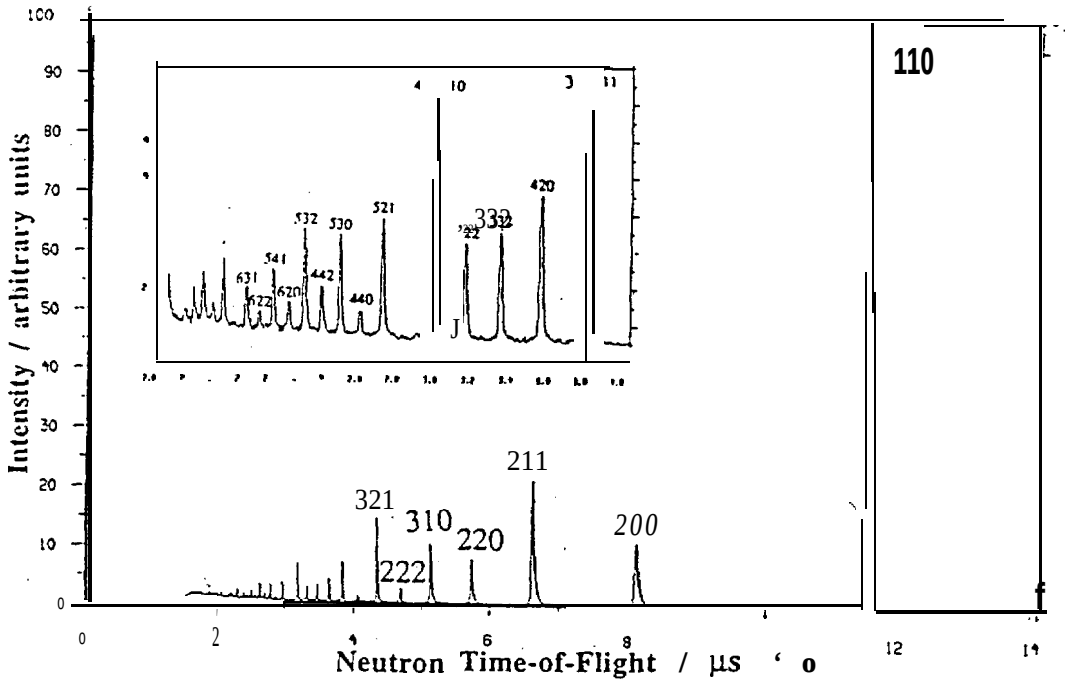

Fig. 2 A typical diffraction profile obtained from ENGIN. The profile was obtained from a mild steel plate used in an experiment to determine the effectiveness of the vibrational stress relief technique. At least 30 diffraction peaks from different atomic lattice planes can be identified.

Since the wavelength λ of a neutron is related to its velocity by the expression:

$$\lambda = \frac{0.39560}{v} \qquad 3.2$$

(when λ is in nm and v in mm/μs) a knowledge of the velocity (v), and the diffraction angle (2θ) is sufficient to determine the lattice spacing d_{hkl} for the particular set of {*hkl*} lattice planes within the sample. Having determined *d*, it is then, in principle, straightforward to calculate the strain (ε) at that point in the sample from the relationship:

$$\varepsilon = (d - d_0)/|d_0| \qquad 3.3$$

where d_0 is the lattice spacing of the unstrained material. It should be noted that the strain (ε) thus measured is a vector quantity and is measured along the direction of d_{hkl}, which is parallel to the vector τ defined by the expression:

$$\tau = k_1 - k_0 \qquad 3.4$$

The directions k_0 and k, being along the incident and scattered directions of the neutron path (see Fig.1)

3.3 *Instrument Construction*

The ENGIN instrument consists of six major components. A collimated incident pulsed neutron beam, a large *xyzω* positioner (to locate the gauge volume within the sample), secondary flight-path

radial collimators (which define the gauge volume), and neutron detectors. In addition two telescopes and a laser/CTV system have been installed to enable the sample to be accurately aligned, and its motion monitored. These components are illustrated schemat tally in Fig. 3.

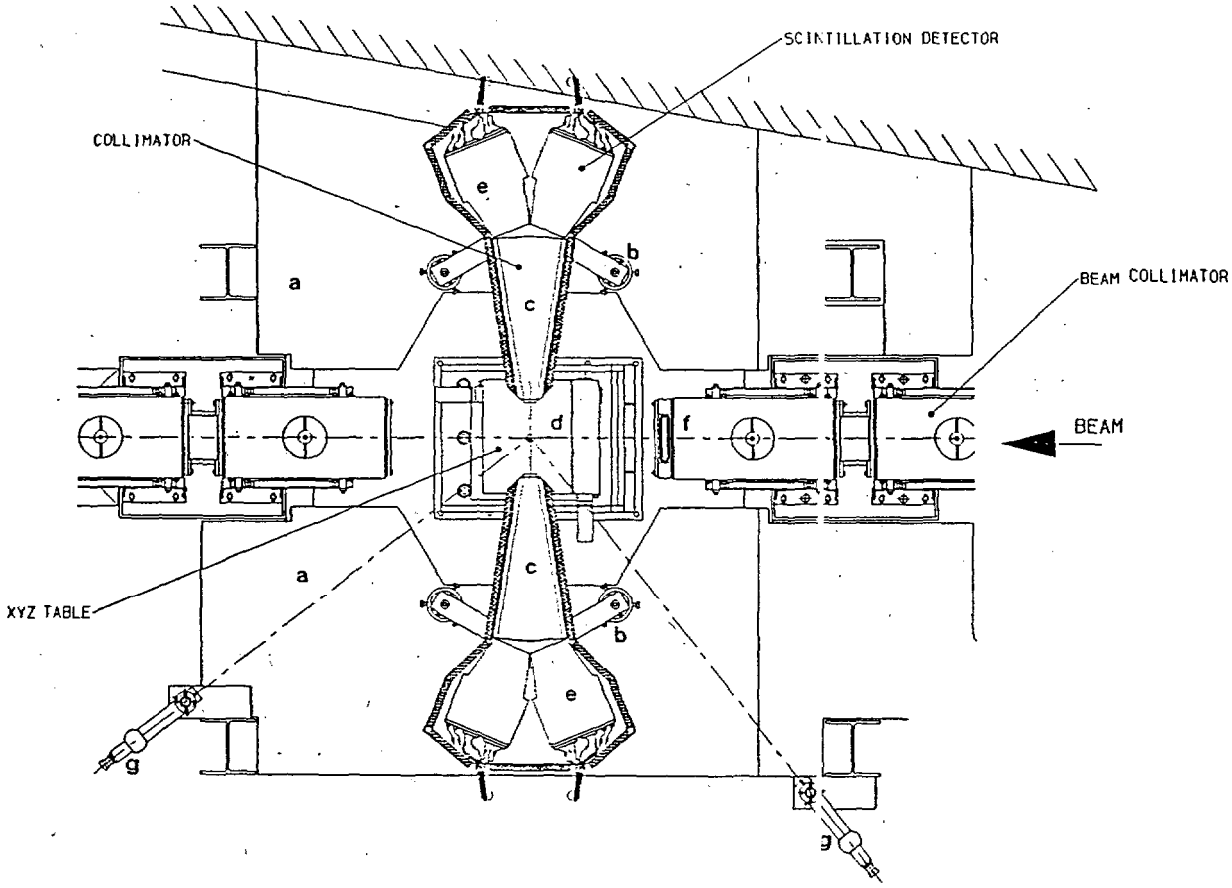

Fig. 3, ENGIN Components

(a) 2 sets of decked steelwork to act as supports for the collimators, (b) 2 rotateable collimator mounts, with alignment blocks (c) 2 radial collimators each with 40 gadolinium oxide coated mylar foils, **(d) An x-y-z-ω positioning** table, (e) Detectors: three rows of 45 detectors stacked above each other. (f) An incoming beam slit definition system (g) Alignment telescopes. Not shown :A closed circuit TV system and class *1* laser is installed to provide a rough marking of the position of the gauge volume.

4 Results

This section presents some of the new measurements made using the ENGIN instrument. In the space available it is not possible to provide a detailed discussion of the software used in analysing the measurements, nor the precise details of the corrections applied. This level of detail maybe found in the Final PREMIS Technical Report.

4.1. Validation *of ENGIN*

As with any new instrument, one of the. first priorities was to evaluate its capabilities and to determine how to achieve the best possible performance. A major part of the validation procedure consisted of measuring a number of standard samples. These are components whose residual strains have been well characterised by measurement at other instruments throughout the world. In addition, numerical modelling has been carried out to predict the expected distribution of internal

strains. The standard samples therefore not only provide a validation of a new neutron instrument against existing installations, but also illustrate how neutron scattering can be used to validate computer codes, for example, finite element modelling (FEM) against experiment. As FEM is becoming an increasingly important industrial design tool, experimental validation of the predictions will become increasingly important.

Measurements on a Diametrically Compressed Ring

A diametrically compressed ring was chosen as a suitable test specimen since it had already been measured at the diffractometers at both the Los Alamos Neutron Scattering Centre (LANSCE) and at Chalk River National Laboratories (CRNL) [7]. The specimen geometry is shown in Fig.4a. This sample provides a reasonably challenging geometry for the finite element code to model, whilst ensuring a smoothly varying residual strain fieId. Furthermore, in this application, good penetration was required to evaluate the strains across the ring radius.

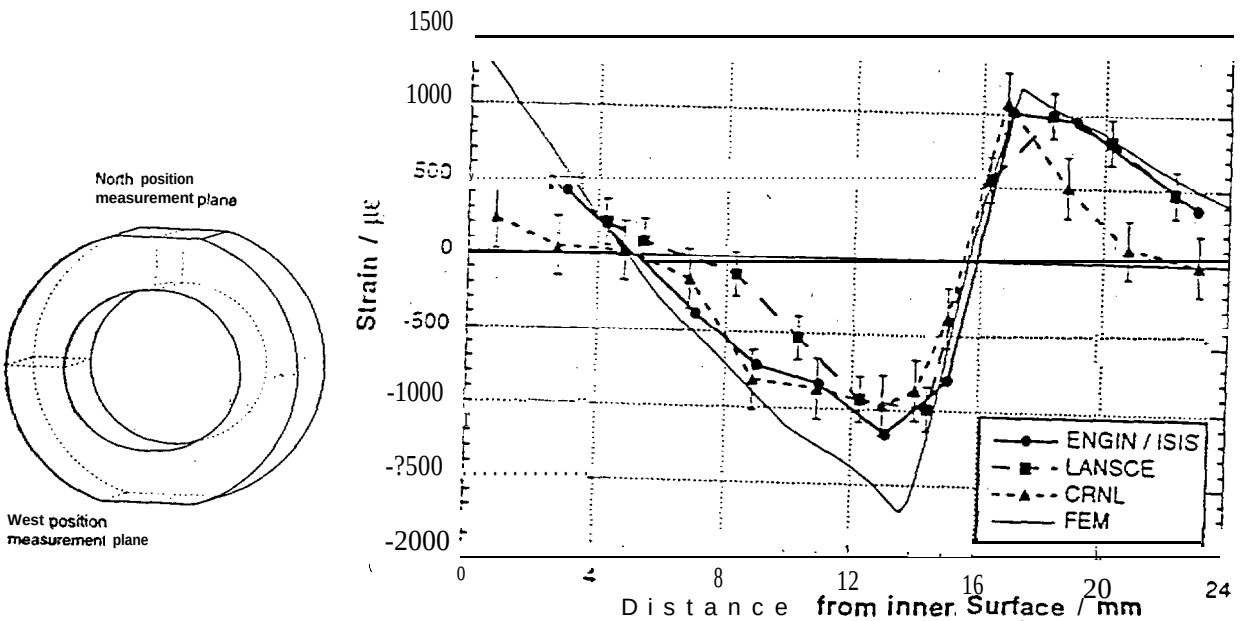

Fig 4. *a) The diametrically compressed steel ring showing the measuring planes, b) The measured tangential residual strains at the* West *position, measured at three neutron sources. The predictions of a finite element computation are also shown [7].*

The ring was made from a 13mm thick austenitic stainless steel (21Cr-6Ni-9Mn) plate. This was given a special thermo-mechanical treatment resulting in a mean grain size of 25 pm, no second phase precipitates and no significant preferred orientation. The circular ring was then machined from the plate and locator flats added. It was then loaded across the locator flats and compressed by 3.4 mm.

A comparison of the three sets of neutron measurements along the ring radius are shown in Fig.4b, alongside the results of a finite element calculation. It is immediately clear that the results from the three instruments are in very good agreement- The measurements from CRNL, are somewhat lower than the other two sets, particularly in the low residual strain region near to the surfaces of the ring. One reason for this is that Chalk River is a reactor source and the strains were deduced from {111) type lattice plane spacing. Since the stiffness of stainless steel is anisotropic, the stiffness of the (111] planes is higher than that of the bulk material The residual stress field therefore generates a lower strain in the {111} planes. On spallation sources, such as ISIS and LANSCE, the lattice strain is

deduced from a number of reflections, so that the measured values are closer to the bulk response. Of course, this difference would not lead to errors in the calculated stress since one would take into account the higher stiffness.

It can also be seen that there is reasonable agreement between the predictions of the finite element model and the experimentally measured results. The predicted lattice strain gradient is somewhat higher, however, especially on the inner half of the specimen. It would of course be interesting to obtain data from other methods of residual stress determination for comparison. However, the nature of this specimen as a standard test piece prevents the undertaking of destructive measurements.

In conclusion, the measurements taken at three neutron strain scanners, representing both reactor and spallation sources, are in very good agreement. This shows that ENGIN in particular and neutron strain scanning in general are capable of achieving a high level of accuracy and repeatability at depths significantly greater than other techniques. The results also illustrate the potential of neutron measurements for the validation of finite element residual stress code.

4.2 ***Stress Relief Procedures***

4.2.1 Introduction

The development of effective stress relief procedures is an important part of many component design processes, and their characterisation requires systematic investigation of the three-dimensional stress state" before and after treatment. Unambiguous determination of the efficacy of thermal and mechanical means of stress relief can be made using neutron diffraction n.

Vibratory stress relief is said to be a method which avoids thermal treatment and the subsequent danger of microstructural changes that may be caused, but it is still an open question how and to what extend the relief takes place and whether the method induces an damage.

4.2.2 *Samples*

For a successful stress relief process using a commercial instrument (in our case a "FOURIERMATIC V.2.01"from VSR) a minimum specimen weight of 50 kg is necessary. A diagram of the sample is shown in Fig.5. A conventional construction steel (German specifics tion: St 52-3) with a minimum yield strength of 520 MPa was chosen-

Three separate samples were produced. In order to achieve an identical initial "as received''stress state for these samples, the production of the rings started from a large 1570 x 1600mm steel plate which was first bent to an "open" pipe with a gap of 33mm. The ends of the pipe were elastically bent together and then the stress state was fixed by welding. Then this pipe was cut into 6 rings with heights of 250 mm.

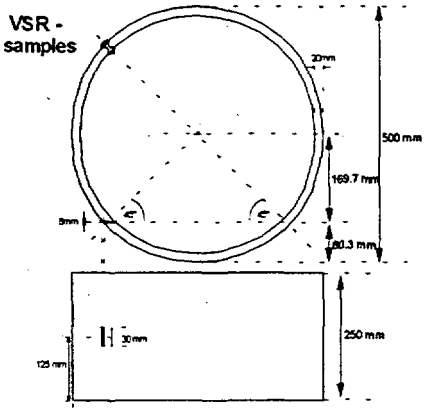

Fig.5 Outlines of the VSR-samples with the size and positions of the machined hole

For the neutron diffraction investigations three of these rings were used. One had no further treatment (AS RECEIVED sample), one got a stress relief heat treatment at 550°C for 5h (HEAT TREATED), and the third one was vibrated by VSR. The steel samples to be investigated were produced according to the requirements of the German company VSR Industrietechnik GmbH., Mühlheim/Ruhr, who also earned out the vibrational treatment.

4.2.3 *Macros tress measurements on ENGIN*

Strain measurements have been performed in the three main directions (hoop, axial and radial) at nine points in different depth of the specimen walls. These positions were named according to the distance from the inner diameter in mm (position 2 to 18).

The diffraction data were analysed using the NISISREF batch refinement routines based on the CCL software at ISIS. The diffraction pattern were refined in the TOF region between 4000 µs and 12500 µs, which includes the bee- reflections (110), (200), (211), (220), (310), (222), (321) and (400).

Using the lattice parameters and the do-values the strain values could be calculated. The literature values of macroscopic elastic constants for ST52-3 were used: E = 207 Gpa, υ = 0.28.

The calculated values are plotted in Figs.6 -8. Using the error of the lattice parameters from the refinement procedure an uncertainty of the stress values of $\Delta\sigma$ = 20 MPa was calculated.

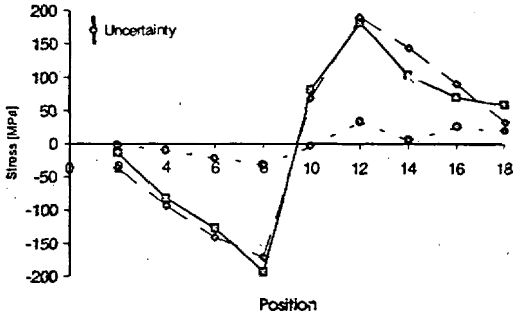

Fig.6: Stress state in hoop direction

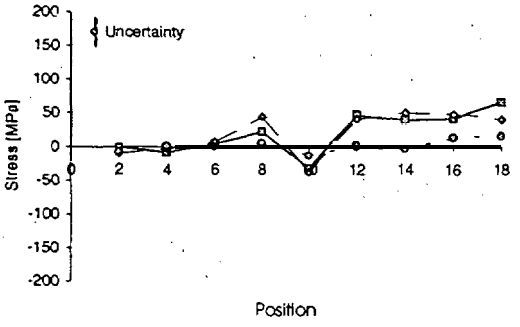

Fig. 7 *Stress state in radial direction*

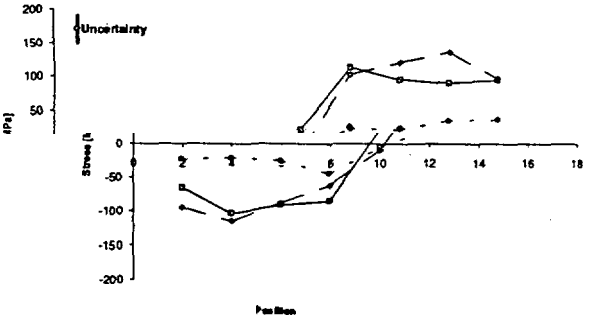

Fig.8 Stress state in axial direction (O heat treated; □as received; ◆vibrated)

In addition to the strain measurements at ENGIN further investigations were made at the Reverse-Time-of-Flight instrument FSS at the research reactor FRG1 in Geesthacht. The aim was to investigate the strain distribution at the ENGIN measuring positions after relief of elastic macrostresses by cutting the sample along the welding seam.

The influence of stress relief treatments on microstresses was alSo looked for by investigating peak widths. The analysis of the data was done by single peak fitting. The RTOF-method used allows peak-fitting with a well determined peak shape function.

4.2.4 Discussion

The measured stress state is mainly caused by two processes during the production of the samples. The plastic deformation from circular shape rolling of the plates results in tensile hoop stresses in the inner and compressive hoop stresses in the outer regions of the ring walls. A similar behaviour is shown for a bending test reported in the liter= ture.

This stress state is overlapped by elastic stresses due to the bending and tacking, which produces a compressive hoop stress in the inner and tensile stress in the outer regions. The measured stress state is a result of the superposition of the plastic and elastic deformation of the rings; the stresses due to the elastic bending being the dominant effect.

The stress calculation shows, that the relatively large strains, which have been measured in radial direction, are cause by Poisson contraction and not by radial stresses.

The neutron diffraction measurements indicate no significant macrostress relief by the vibrational treatment. If the errors of the measurement are taken into account, it can be said that the results in all three directions give the same value for the 'as received' and vibrated sample. Most investigations on vibrational stress relief show similar results.

On the other hand the heat treated sample is almost stress free. In all directions the values of residual. stresses smaller than 50 MPa were found. Thus the neutron diffraction measurements show an almost complete stress relief by the heat treatment.

Another point of the investigation of the vibrational stress relief procedure should be a possible change in the microstresses, which have an influence on the peak shape and width which are parameters of the Rietveld refinement. From the analysis of the actual data no significant changes in the peak shape parameters were found.

The macrostrains resulting from the FSS-measurements show the same effects of the stress relief procedures as the ENGIN-measurements. Macrostress relief is only found for the annealing process, but not for the VSR-treatment.

The most interesting part of these investigations was the peak widths measured as Gaussian parameters fitted to single peaks. It was hoped that the assumed effect of the VSR-treatment on dislocation distributions could be found in smaller peak widths for the VSR-treated sample. This effect was not observed in these measurements.

4.3 *Measurement of the Residual Stresses at a Cold Expanded Hole*

4.3.1 *Introduction*

Rising demand for longer lives in both civil and military aerospace is likely to ensure that the economical lives of some aircraft structures will be dictated by their long-term fatigue performances. Generally, the primary source of fatigue damage (cracking), is at mechanical joints and the problem becomes more vital as the demand for minimum structural weight to improved aircraft performance **increases.**

Cold expansion techniques have been used for over thirty years to produce fatigue life enhancement and have been reviewed by Champoux[Champoux 1986]. Superposition of the residual stresses near the hole with service loads leads to improvements in fatigue life either by delaying or suppressing crack initiation or more often by reducing fatigue crack growth rates. Expansion is achieved using prescribed levels of mandrel interference. The optimum degree of mandrel interference for a particular application will however depend. on the local geometry of the component and fatigue life predictions of structures containing such expanded holes rely critically on estimates of the residual stress distribution surrounding the hole. Increasing importance is being given to the three dimensionality of the residual stress distribution produced by split sleeve expansion. It has been suggested from fractographic evidence that the residual stress distribution varies across the thickness

of the plate [Ozelton 1989 and Pen 1989]. In particular it has been suggested that a larger residual compressive hoop stress is generated at the mandrel outlet face of the plate than at the mandrel inlet face.

Work at the Open University using the ENGIN instrument has provided the first 3D residual stress measurement around a cold expanded hole. Data of this type are essential if the locations and growth rates of fatigue cracks near expanded fastener holes are to be modelled reliably.

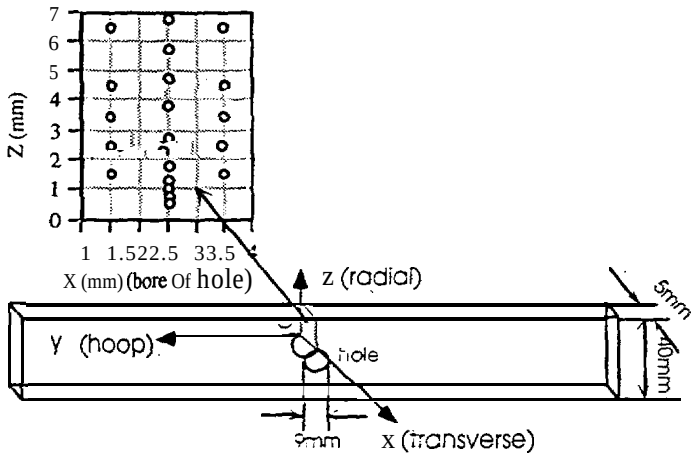

Fig. 9 Dimensions of the cold expanded hole component

4.3.2 *Precise Determination Of Measurement Position*

In order to obtain the highest precision a number of careful measurements were carried out to precisely determine the position of the gauge volume with respect to the specimen surfaces. The full stress tensor approach used here also required measurements to be made accurately along the three principal axes which were known due to the symmetry of the hole expansion process.

To achieve the former condition the position of the gauge volume with respect to the component was calculated to an accuracy of 0.1mm by fast surface scanning and fitting the resulting data to a model of the intensity variation as the gauge volume enters the material.

4.3.3 ***Stress*** *distribution around the cold expanded hole*

The dimensions of the component are shown in Fig.9. A series of measurements of the hoop and transverse strains were made, along the zx plane at the positions shown in Fig.9. The frame and hence the specimen was then rotated by 90^o and measurement of the radial and transverse strains were made at the same positions in the zx plane of the component. The refinement of all the runs was carried out using a Pawley refinement- Thus the residual strain distribution is represented by the least-squares average (LSA) strain, e.g. the strain calculated by

$$\varepsilon = (\Delta a)/a_0 \qquad 4.1$$

where Δa is the lattice parameter shift, and a_0 is the strain-free lattice parameter. Fig.10 shows the residual strain distribution along the mid-thickness of the plate. The strain-free value, a_o, was obtained by measuring a point 100mm away from the hole.

The stress distribution in isotropic polycrystalline materials is calculated from the measured strains by

$$e_{ij}^{(hkl)} = \frac{1}{2} s_2^{(hkl)} \sigma_{ij} + \delta_{ij} s_1^{(hkl)} \sigma_{kk} \qquad 4.2$$

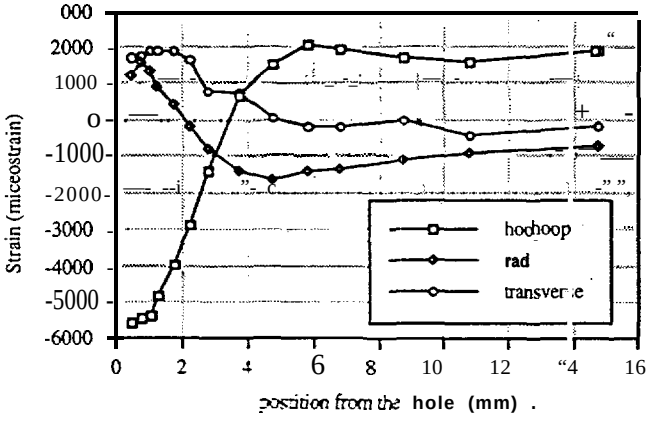

Fig. 10 Residual strain distribution along mid-thickness of the plate.

where the elastic constants $s_1^{(hkl)}$ and $\frac{1}{2}\ s_2^{(hkl)}$ are defined as

$$s_1^{(hkl)} = (\ldots)^{(hkl)} \qquad \text{and} \qquad \frac{1}{2}\ s_2^{(hkl)} = \left(\frac{1+\nu}{E}\right)^{(hkl)} \qquad 4.3$$

The residual stress distribution has been calculated from the strain distribution measured by neutron diffraction, using equations 4.2 and 4..3 assuming that:

- the three measured directions coincide with the principal axes of the'component.
- the aluminium plate is an isotropic polycrystalline material.
- the LSA strain could represent the bulk property of the aluminium plate
- the effect of texture is negligible

It can be seen from Fig.11 that the general shape of the residual stress distribution is as expected and shows reasonable correlation with previously published estimates of the distribution obtained form destructive mechanical tests except that there was no evidence of stress relaxation near the hole. The accuracy of these measurements is dependent on how well we can control or compensate for systematic errors. The peak positions and hence the lattice parameter; may be affected by a greater or lesser degree by type I, 11 and III residual stresses, prior plastic deformation and instrument effects. In this analysis we will focus on the likely affects of any speed ic instrumental effects and the use of a gauge volume which is large compared to the scale of the residual stress gradient,

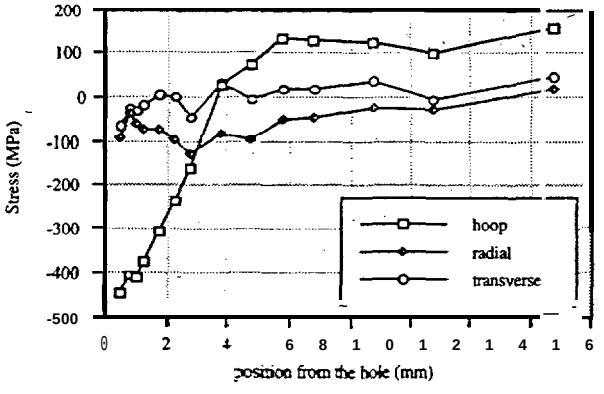

Fig. 11 Residual *stress distribution along the mid-thickness*

4.3.4 Correction for Surface Effects

A 'pseudo-strain' may be measured when the gauge volume straddles the sample surface so that only part of the collimating detector sees all of the gauge volume. For the case of the cold expanded

hole in the aluminium plate only the radial strain measurement was affected as the other strains were measured by scanning the gauge volume vertically through the component surface. In this analysis an empirical instrumental correction was used, based on the knowledge that the radial stress should become zero as the surface is approached.

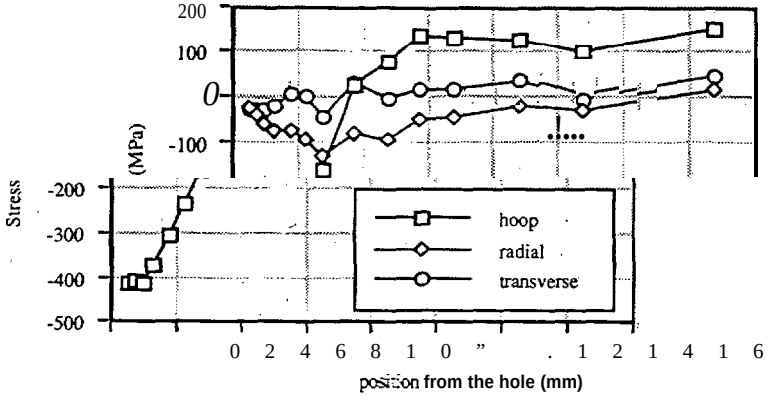

Fig. 12 Residual stress distribution after correction

The corrected results of the residual stress distribution along mid-thickness line is shown in Fig.12. Although the residual stress distribution is substantially unchanged there is now some evidence of stress relaxation near the hole. Based on these corrected results and in combination with surface residual stress measurements made by X-ray a 3D hoop residual stress map may be constructed using the principal of minimum curvature and is plotted in Fig. 13.

4.3.5 *The Effect of Gauge Volume Averaging on Interpreting Strain Gradients*

The averaging effect of the gauge volume only affects the measured strain distribution in areas of highly strain 'gradients, such as near the hole in the cold expanded plate. This is why the evidence of hole relaxation seen in the neutron measurements is not as pronounced as in the mechanical measurements made *using the* modified Sachs technique (Fig.14).

An interesting comparison maybe made by comparing the measured neutron distribution with the distribution produced by *averaging the* Sachs strain distribution over a similar gauge volume size, Fig.15 shows a 3D plot of the stresses calculated from an *average* of the Sachs values. Comparing Fig.13 with Fig.15 shows the **excellent** agreement between the two techniques.

4.3.6 *Summary*

- The first 3-D stress measurement has been made at a 4% FTI expanded hole in high strength aluminium alloy using neutron diffraction.
- Differences in residual compressive hoop stress distribution were detected through the thickness of the specimen" with hoop stresses being smaller at the 'inlet', side of the hole, (where, the mandrel first engages), when compared to the 'outlet' side, similar to the result from mechanical measurement.
- The comparison between the measurements from neutron diffraction and modified Sachs method is feasible providing the gauge volume average effect in neutron diffraction is taken into account
- The variation of peak width can be used as an indicator of variation of type I strain gradients in the materials.

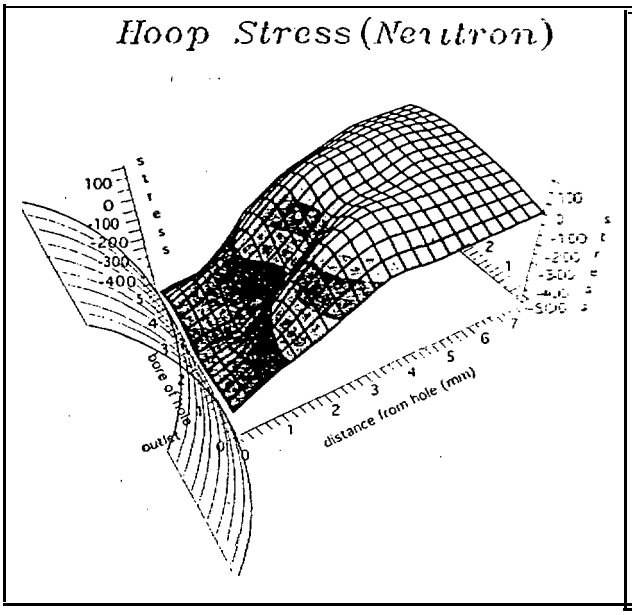

Fig. 13

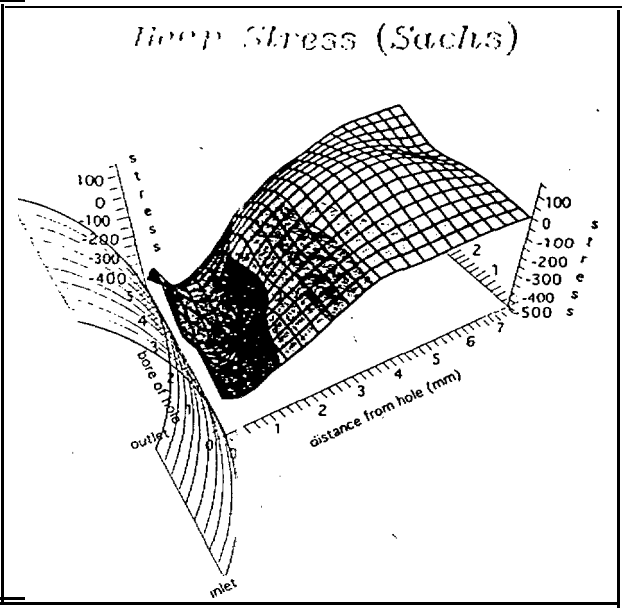

Fig.14

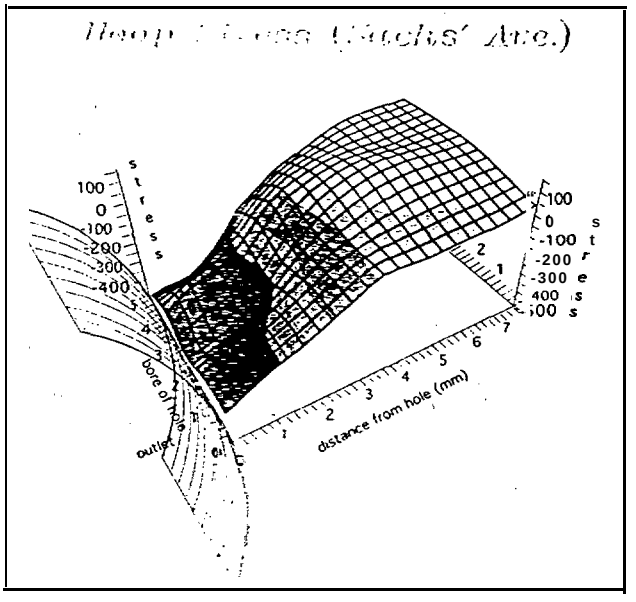

Fig. 15

4.4 *SURFACE MEASUREMENTS*

Arguably the most important region of a component, as far as residual stresses are concerned, is the 'near surface region. Cracks most often nucleate at surfaces for a nun-d ber of reasons. Machining will leave many surface defects which may act as crack nucleation sites. Bending loads applied to the specimen will result in stress maxima which, if tensile, can acc elerate crack nucleation -and propagation. By introducing a compressive residual stress into the surface region the effective stress intensities at the crack tips are reduced and crack growth is therefore inhibited .[8]. Surface treatments such as shot peening are therefore very important (see Fig. 16). The ability of neutrons to non-destructively measure the residual stresses not only at the surfa :e, but also further within the specimen where the residual stresses will be tensile and 'therefore potentially life-limiting represents a unique advantage of neutron strain scanning over other methods.

A shot peened sample of a titanium alloy was obtained from Rolls Royce in order to measure the residual stresses as a function of depth ,[9]. Ti alloys are among the most challenging because they absorb neutrons strongly and scatter a substantial fraction of the neutrons incoherently.

The specimen plate, measuring 23 x 19 x 51mm was shot peened on one surface using 230R to an intensity of **20A. Measurements** *were* taken at nine depths **beneath the surface in** order to build up good picture of the residual strain field in a reasonable measuring time. The measuring volume sampled by the neutrons was 0.5 x 1.4 x 25mrn, with the 0.5mm dimension being parallel to the surface normal. The specimen was mounted with the surface parallel to the neutron beam (horizontal) and seamed vertically to record the strain as a function of depth.

The in-plane and normal strain measurements are shown in Fig.17 as a function of depth. The quality of the data is immediately obvious. Comparable X-ray measurements would be confined to a very small region (a few pm for Ti) close to the surface of the specimen because of the high absorption of heavy elements. The overall shape of the curve is very much as expected and it has even been possible to resolve the fact that the maximum compressive residual stress lies somewhat beneath the surface. The deep tensile maxima has also been recorded. It is worth emphasizing that whilst neutrons are most frequently utilised for their penetration power, which enables them to make measurements deep within components, here we see that ENGIN can be used to successfully and accurately measure residual strains at a distance of only 80pm from a surface, in a very difficult material, with sensibly short measurement times.

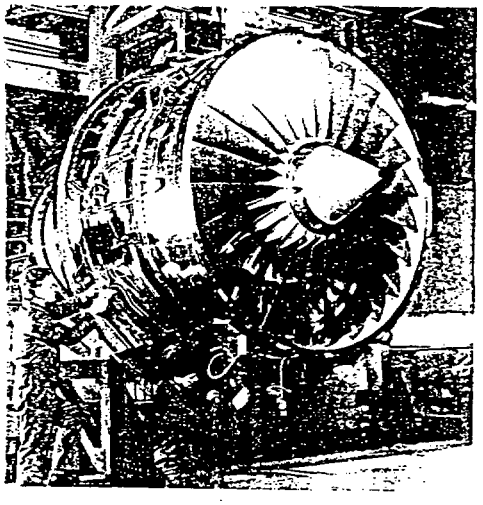

Fig.16 Shot peening is a particularly important process for improving fatigue life in components such as the titanium alloy fan blades on the RB211 engine shown above.

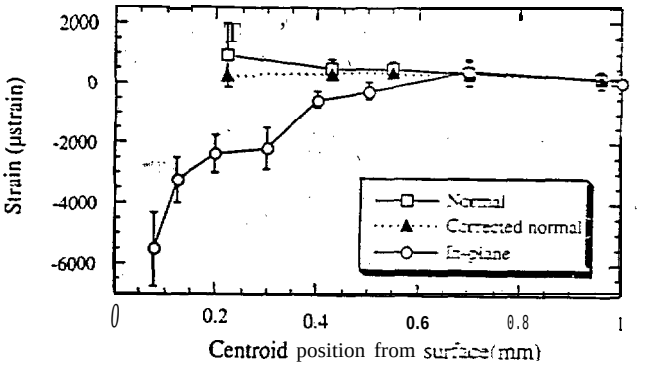

Fig. 17 Residual strains near the surface of a shot peened sample of IMI 318 Titanium alloy as measured on ENGIN. The strain field is measured to within 80μm of the surface.

4.5 *MULTI-PHASE MATERIALS*

Neutron strain scanners, especially those situated on spallation sources, are ideal tools for measuring the internal stresses within multi-phase materials. This is because the various phases diffract into different Bragg peaks, so that the response of **each** phase can be evaluated separately. The diffraction elastic constants (essentially components of the single crystal compliance) may then be used to convert the measured strains into the corresponding stresses. Pulsed sources are particularly well suited to such studies because the complete diffraction profile is measured at one time rather than peak by peak. The peaks corresponding to different phases may thus be analysed separately, using Rietveld profile analysis [10] to provide a measure of the stresses in **each** phase.

Metal matrix composites are two phase *systems* of increasing impc rtance. The introduction of a reinforcing ceramic phase into a metallic matrix enables a high spec fic stiffness and strength to be achieved, whilst retaining many of the attractive features of the ori inal matrix material. Because composites are inherently inhomogeneous, internal stresses develop when they are loaded or when the temperature is changed. As the term reinforced implies, the pi operties of these materials are heavily dependent on the distribution of stresses between the phases. For this reason, neutron strain measurements have been instrumental in establishing our understand ng of these materials.

Metal matrix composites vary in design and price from low cost, low temperature Al/SiC particulate materials to high cost, high temperature Ti/SiC continuous fibre composites for performance applications, such as use in aeroengines. Irrespective of the type, the key to achieving improved performance is an effective transfer of load from matrix to reinfo cement during loading, while controlling the effect of thermal residual, or thermal cycle induced, s resses. Both these aspects can be effectively monitored using neutron strain scanning.

A good example of such a study is that undertaken by Withers & Clarke [11] on Ti/35%SiC aligned continuous fibre composite at Chalk River. Here the variation of the internal strains was evaluated in both phases as a function of the applied load and the plastic strain and the results are shown in Fig.18. As is clear from the corresponding macroscopic stress stra n curve, the applied load was progressively applied and after each step the strains evaluated. Mess urements were also made after unloading at various stages to identify the development of the residual strain with plastic straining. The initial strain values are the result of thermal residual stresses wit hin the composite. These arise because the composite is fabricated by a fibre/foil technique at high temperature (950°C). As one would expect, given that Ti has'a larger coefficient of thermal expansion than SiC, the SiC fibres are found to be in residual compression, the matrix tension. These strain: are equivalent to those caused by a temperature drop of around 81O"C and represent thermal stress s of about -720 and 360MPa in fibres and matrix respectively. This indicates that most of the rni fit generated upon cooling is . elastically accommodated.

Fig. 18 shows the axial strains in a continuously fibre reinforced Ti-6Al-4V/35%SiC composite subjected to incremental plastic straining. The loading sequence is shown on the left hand side of the graph.

Not surprisingly, as the applied load is increased, the strains in both phases become tensile. Furthermore, at high applied loads, the SiC curve can be seen to flatten quite significantly, i.e. the rate of SiC fibre loading increases. This occurs at the point when the macroscopic stress strain curve first exceeds the proportional limit. This is due to the onset of plastic deformation of the matrix which, though not recorded directly because diffraction is sensitive only to elastic strains, causes a transfer of the applied load from matrix to fibres and hence a decreas 2 in the rate of elastic straining of the matrix and an increase in that of the fibres. Upon unloading, tne transfer of load towards the fibres caused by the plastic deformation of the matrix is clearly seen. Here composite plastic strains of less than 0.2% have increased the fibre stress by around 400MPa.

4.6 **THERMAL CYCLING** *MEASUREMENTS*

In the last section we saw how neutron strain measurement can provide insights into the internal stress response to the application of an applied load. But another important area which illustrates the versatility of the technique is the monitoring of the development and relaxation of thermal stresses. This might be the thermally activated relaxation of long-range stresses in large engineering components, such as the plastically' formed ring of section 3, or the development of internal stresses in composite materials. In the former case, direct real time measurements enable the optimisation of stress relief treatments. In the latter case, the development of internal stresses in composites is of great commercial importance, because of the marked effect thermal stresses can have in satiations where the temperature is cycled. Thermal cycle-induced effects include the progressive distortion of components and the occurrence of superplastic extensions under very low applied loads. Cycling environments include high temperature cycling régimes typical of aeronautical and automotive applications and cryogenic cycling experienced in space applications. The behaviour of MMCS under thermal cycling is therefore an important area of research.

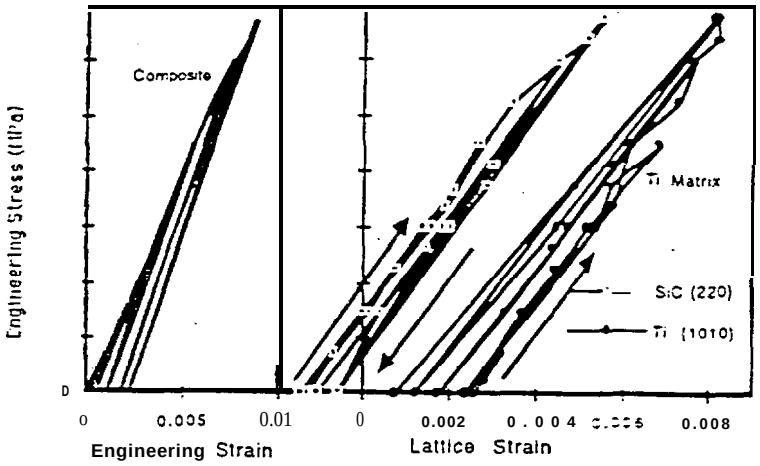

Fig.18 The matrix and fibre internal strain response for Ti-6Al-4V/35%SiC fibre composite, plotted along the macroscopic stress strain curve.

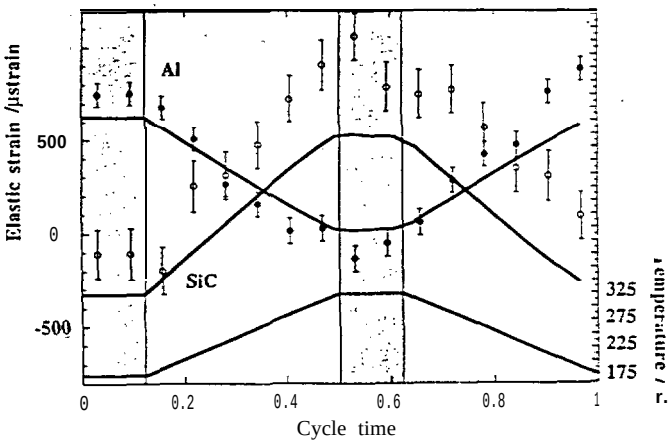

Fig. 19 Comparison of the variation of neutron diffraction determined non-thermal strains (i.e.-α AT) in the two phases of the composite during the 175-325°C cycle with results from finite element modelling.

The basis of these effects is not difficult to identify. Even for small changes of temperature, thermal expansion mismatch stresses can be sufficient to cause localised yielding in the matrix. With repeated thermal cycling, this plastic increment can accumulate, resulting in large macroscopic plastic strains. If a small external load is applied simultaneously, net plastic strains of many hundred percent can be accumulated. This superplastic behaviour is of particular interest for the forming of MMC components .[12]. Despite the enormous importance of the internal stresses in driving these behaviors, it has not been possible to measure the development of these stresses directly.

Neutron diffraction studies have been precluded to date because of the lengthy data accumulation times (around 1hr for typical measurements) in comparison with the period of typical thermal cycles (normally -5-15 mins, since this leads to convenient experiment lifetimes when the cumulative effect of many consecutive cycles are to be studied microscopically). Previous neutron studies of thermal cycling have therefore involved long dwell periods in order to acquire significant data .[13]. However a novel stroboscopic technique, developed on ENGIN, involving software binning enables 16 distinct measurements to be made for thermal cycles lasting only a few minutes.

The technique relies on the fact that the behaviour of the specimen does not vary over very many consecutive cycles .[14, 15]. A number of data "bins" are used to store the profiles in memory, each of which contains only those neutrons which were detected during a specific "section of each cycle. As the cycle progresses, the bin into which the detected neutrons are recorded is periodically incremented. At the end of the cycle, the bin counter is reset and the next thermal cycle begins. Typically 16 bins are used to adequately cover a whole thermal cycle, although this maybe reduced to 8 if required.

Fig.19 shows the axial elastic strain recorded in both reinforcement and matrix of a 10vol% SiC whisker reinforced commercially pure Al composite at 16 intervals during thermal cycling between 175-325°C ,[16]. The period of the cycles was 800s and the data represents the aggregate of over 150 cycles. The material was produced by a powder route and extrusion method- The specimen was subject to a load of 25MPa throughout the course of the experiment. The solid lines represent the results of an independent finite element model of the composite ,[17].

These results are the first direct measurements of the variation of internal strains during continuous thermal cycle fatigue in a composite system and can be understood in terms of the generation and

relaxation of thermal misfit as the cycle proceeds. As the temperature is increased the strain in the Al, which has a higher CTE than that of SiC, becomes more compressive, while the strain in the SiC becomes correspondingly more tensile. In this context it is irnportar t to note that the stress free expansion of each phase has been accounted for so that the strain than ges summarised in Fig.19 are solely those arising as a direct result of the internal stresses. Furthermore, it can be seen from the graph that the FEM model successfully predicts the rate of rise of the internal strains of the two phases with temperature.

During the dwell for 100s at the maximum temperature the experimental results for both phases show that there is a marked decrease of internal strain during this period. This is caused by creeping of the Al matrix in order to reduce its strain energy. The SiC does not creep, but its strain must also decrease in order to maintain load balance between the two phases. The FEM predictions do not show such pronounced creep effects, indicating that the model underestimates the level of creep at high temperatures. Upon cooling the strain changes reverse and are seen to change at approximately the same rate as they developed during heating. This indicates that the majority of the thermal misfit is elastic.

At the temperature where the stresses in the two phases are equal, there is no strain mismatch and the specimen is termed "stress free", although there will still be the 25MPa stress due to the external loading. The stress free temperature assumed in the finite element model was 250°C. The average measured stress free temperature between the heating and cooling ramps is 268°C. The difference between these two values may explain the differences in' the absolute values of the strains between the FEM model and the experimental measurements.

5 CONCLUSIONS

ENGIN is proving to be a versatile and capable tool for the measurement of both macroscopic and micrsocopic phase strains and hence stress-es, in both static and dynamic environments. The results described here demonstrate just some of the opportunities for new scientific and engineering research, The future will no doubt see a large expansion in the scope of such measurements. ENGIN has now taken its place alongside other available instruments at the Rutherford Appleton Lab.

6 ACKNOWLEDGEMENTS

This work was carried out under an EC Brite/EuRam programme No. BRE2-CT92-0156 "PREMIS" (PREcise Measurement of Internal Stress). The authors wish to thank Tom Holden, VSR Industrietechnik GMBH and Rolls Royce Plc for providing specimens used for this study. Many thanks also to Mark Daymond, Jörg Larsen, Carsten Ohms and David Wang for obtaining much of the data presented in this paper.

7 REFERENCES

1. C.C. WILSON, Neutron News. 6 (2) (1995).

2. A.J. ALLEN, C. ANDREANI, M.T. HUTCHINGS and C.G. WINDSOR, NDT International. (October 1981) p. 249-54.

3. M.T. HUTCHINGS, in Measurement of Residual Stress Using Neutron Diffraction, Ed. M.T. Hutchings and A.D. Krawitz, Kluwer Acad Pub: Netherlands (1992), p.3-18.

4. M.W. JOHNSON and W.I.F. DAVID, Rutherford Appleton" Laboratory Report, RAL-85-112, (1985).

5. N.J. RHODES, Proc. ICANS XII, in Rutherford Appleton Laboratory Report, RAL-94-025, (1994).

6. W.I.F. DAVID and J.D. JORGENSEN, in The Rietveld Method, Ed. R.A. Young, OUP, (1995).

7. T.M. HOLDEN, B.R. HOSBONS and S.R. MACEWEN (1992), in Measurement of Residual Stress Using Neutron Diffraction, Ed. M.T. Hutchings and A.D. Krawitz, Kluwer Acad Pub: Netherlands (1992), p. 93-112.

8. M.E. FITZPATRICK, Thesis, Cambridge University, (1995).

9. D.Q. WANG and L. EDWARDS, in Brite/EuRam Report BRE2-CT92-0156 PREMIS/95/R7 (1995).

10. W.I.F. DAVID, R.M. IBBERSON and J.C. MATTHEWMAN, in Rutherford Appleton Laboratory Report, RAL-92-032 (1992).

11. P.]. WITHERS and A.F'. CLARKE, Personal communication (1995).

12. T.W. CLYNE and P.J. WITHERS, An Introduction to Metal Matrix Composites, Cambridge University Press, Cambridge, (1993).

13. P.J. WITHERS, D.J. JENSEN, H. LILHOLT and W.M. STOBBS, Proc. ICCM VI/ECCM2, vol. 2, Ed. F.L. Matthews, et al. (1987), p. 255-264.

14. S.M. PICKARD and B. DERBY, Acts Metall. 38, (1990), p. 2537-2552.

15. M.Y. WU and O.D. SHERBY, Scripts Met. 18, (1984), p. 773-776.

16. M.R. DAYMOND and P.J. WITHERS, Int. Conf. on Composite Materials 10, Whistler Vancouver, Canada, Ed. A. Poursartip, et al., (1995).

17. M.R. DAYMOND and P.J. WITHERS, Mat. Sci. Tech. Accepted for publication. (1995).